

Meter-scale High-temperature Superconducting RF Waveguides with Integrated Filters and Attenuators

Vyacheslav Solovyov, Hyunwoo Kim, Dmytro Nykypanchuk, and Paul Farrell

Abstract— We report the performance of coplanar, multifilament waveguides manufactured from crystalline films of a well-known HTS compound, YBCO, transferred to a low-loss dielectric substrate, such as E-Kapton. The coplanar two-line waveguide delivers low cross-talk, below 20 dB level, and low attenuation, below 4 dB/m at 6 GHz, 77 K. Controlled-impedance 50 Ω waveguides would require a method for reliable patterning narrow, less than 100-micron wide, YBCO traces over a meter length. We report a lithography-etching approach that minimizes the difference in the etching rate of YBCO and the metallization layers of Ag and Cu. An array of metalized vias isolates the traces. We describe the via metallization process that is not damaging to YBCO and compatible with dense, 2 mm period, arrays of vias.

Index Terms— High-temperature superconductors, quantum computing, RF properties, scalable interface.

I. INTRODUCTION

THE SUCCESS of the quantum computer industry depends on an economic scale-up of the superconducting quantum systems (sQS). Currently, sQS are considered to be input-limited systems suitable for computational tasks that can tolerate low-bandwidth input [1]. The input is realized by multiple RF and DC lines which are the most prominent features of a quantum computer and occupy a major part of the cryostat volume. Additionally, the RF signal needs to be conditioned by attenuation and filtering [2]. The discrete filters and attenuators add to the system volume and thermal mass.

In our previous works [3, 4] we have demonstrated that the epitaxial YBCO films, grown on metal substrates, can be transferred onto a dielectric substrate without degradation of superconducting properties. The YBCO-Kapton laminate was shown to be compatible with multi-layer RF structures, such as strip lines and metalized vias. A low-resistance, below 100 n Ω cm² solderable contact to YBCO can be easily made using the Ag diffusion layer [5]. A much higher transition temperature and easy solderability are practical advantages of YBCO material over Nb and Nb-Ti.

YBCO, with T_c over 90 K, allows for a seamless transition from the 60 K state to the mK environment, thus eliminating intermediate connectors. The passive and active surface-mounted devices (SMD) can be soldered on the waveguide traces to realize integrated signal conditioning components. Fig. 1 is a rendering of the proposed integrated interconnect. The

metallization overlayer, comprised of 20 μ m of copper and 1 μ m of silver diffusion layer, remains in thermalized portions of the cable, where surface-mounted devices (SMD) are to be mounted by direct soldering onto the copper layer. The metallization is removed in the parts of the waveguide between the cooling stages, creating an area with ultra-low thermal conductivity or thermal break. The thermal break blocks heat from traveling between the cooling stages.

Realizing such a concept would require a continuous YBCO waveguide over 1 meter in length. The 2G conductors are currently offered as continuous 12 mm wide coupons over

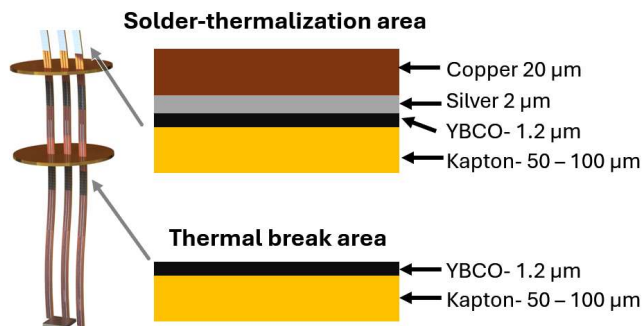


Fig. 1. Rendering of the proposed microwave interconnect. The metallization remains in the parts of the cable where thermalization is needed or SMD components are to be soldered. The metal overlayer is removed in sections of the cable between cooling stages.

100 m long [6], with a certified critical current density. It is well-recognized that 2G conductors contain multiple microscopic defects [7] that often remain undetected by the quality-control methods employed by the 2G manufacturers, such as the scanning Hall probe array method (so-called TapeStar) [8]. A defect smaller than 1 mm may not matter in a wide, 4 mm tape since the supercurrent has room to flow around. However, a 50 Ω impedance-control microstrip would need a signal line less than 1 mm wide; even narrower lines would be required in fully shielded waveguides.

Here, we show that the YBCO film deposited by the Chemical Vapor Deposition (CVD), which is currently employed by SuperPower Inc., is suitable for manufacturing up to 1-meter-long impedance-controlled waveguides, that can also be integrated with low-pass filters and attenuators.

Hyunwoo Kim and Paul Farrell is with Brookhaven Technology Group, 1000 Innovation Road, Stony Brook, NY 11794 (hkim@brookhaventech.com and pfarrel@brookhaventech.com).

Dmytro Nykypanchuk is with Brookhaven National Laboratory, Upton, NY 11973 (dnykypan@bnl.gov)

Color versions of one or more of the figures in this paper are available online at <http://ieeexplore.ieee.org>.

This work was supported in part by U.S. DOE Office of Science awards DE-SC0021707, and DE-SC0012704. (Corresponding author: Vyacheslav Solovyov.)

V. F. Solovyov is with Brookhaven Technology Group, 1000 Innovation Road, Stony Brook, NY 11794, (slowa@brookhaventech.com).

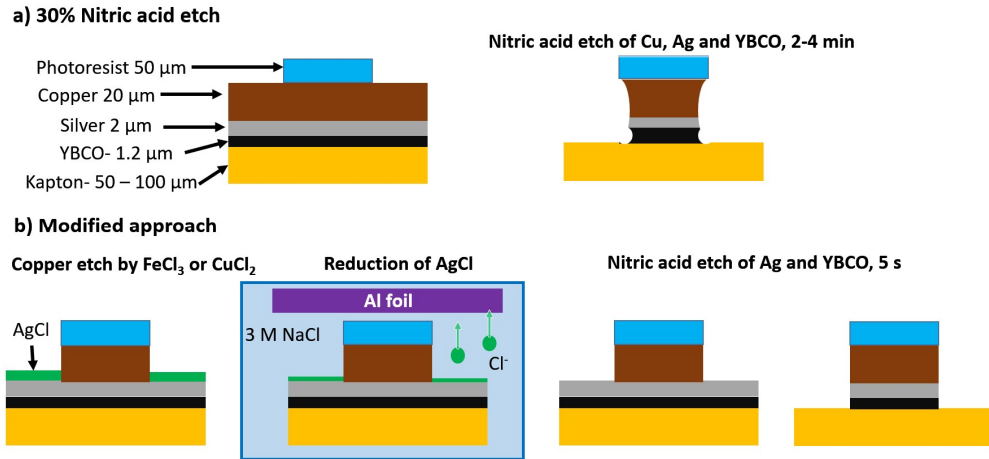


Fig. 2. a) Development of the waveguide trace using the concentrated (20%) nitric acid etch. The process does etch the whole stack. However, a significant under-etch often occurs due to the much faster etching of copper than silver. b) The modified approach employed in this work is to remove copper using either FeCl_3 or CuCl_2 etch. The process leaves a silver layer covered with insoluble AgCl. AgCl is reduced to metallic silver using the exchange reaction with the aluminum metal, followed by a 5 s nitric acid etch.

II. EXPERIMENT

The 12 mm wide YBCO films, supported by 20 μm thick copper foil, were separated (exfoliated) from the metal substrate and buffer of 2G tapes supplied by SuperPower Inc. [9]. After the lamination step, a custom drilling machine drilled the 0.5 mm diameter via bores. The machine was equipped with a digital camera that automatically recognized the tape edge and drilled a pre-programmed hole pattern. The vias were metallized by electrolytic deposition of copper and protected by a UV-curable solder mask, as described earlier [4].

Unless otherwise stated, Stycast 1266 epoxy was used for laminations. A separate patch of laminations was performed using DuPont b-staged acrylic (Pyrallux® LF) and epoxy (Pyrallux® HP) dry film adhesives, processed in a hot press (170°C, under 1.3 MPa) for 1 hr. These samples were analyzed

using X-ray diffraction using the Rigaku SmartLab system equipped with an X-ray mirror.

The trace pattern was developed by contact lithography. In the prior work, we etched the pattern in 20% Nitric acid solution for 2-4 min [3], Fig. 2a. The method worked well as a one-step development of relatively wide, over 1 mm, traces of Cu-Ag-YBCO stacks. For narrower traces, the faster etching rate of copper resulted in multiple trace breakages. Schematically shown in Fig. 2b, an alternative processing sequence eliminates this problem by separating copper and silver etches. First, copper is removed by CuCl_2 etch. The CuCl_2 etch was chosen because it is the industry standard for printed electronics manufacturing and is proven to deliver copper features with better than 10 μm resolution. The problem was that CuCl_2 reacted with silver, forming AgCl coating, which was insoluble in acidic etchants. A separate step was therefore introduced to reduce the AgCl coating through an exchange reaction with Al metal, Fig. 2b. The sample was placed in a bath lined with Al foil and filled with an aqueous solution of 3M NaCl at 50°C. After 5 min, the AgCl layer was fully converted to Ag, which was detected by the coating color change from gray (AgCl) to white (Ag). Next, very fast, only 5 s, immersion into 20% nitric acid was sufficient to remove the remaining silver layer and YBCO. This procedure ensured sharp features with practically no loss of traces.

Fig. 3a is a photograph of 20, 40, and 100 cm long co-planar waveguides manufactured using the described process. At approximately 5 cm on each end, the original metallization was left intact for soldering of edge-mount SMP terminations, Molex model 0734153591. Fig. 3b shows the design of a low-pass filter integrated with a 15 dB attenuator. The filter was designed using Keysight ADS studio. The attenuator was realized as an unequal power divider using 0603 SMD resistors. The waveguides were tested at 77 K in liquid Nitrogen using a Signal Hound scalar network analyzer comprised of a TG-124A generator and SA-124B spectrum analyzer. The analyzer was

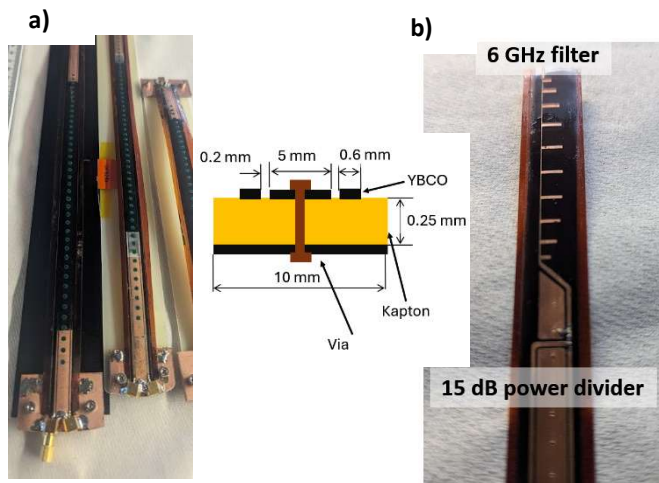


Fig. 3. a) 40 and 100 cm long YBCO-Kapton waveguides terminated with in-line SMP connectors. The via pads are masked with green solder mask. The inset shows cross-section of the waveguide. b) A 6GHz low-pass filter and 15 dB attenuator integrated with a waveguide.

calibrated at 77 K using the Short-Open-Load-Through (SOLT) method.

III. RESULTS AND DISCUSSION

Fig. 4a presents the results of 77 K tests of 40 and 100-cm long waveguides shown in Fig. 3a. A short, 1-cm long waveguide performance is also included to separate the contribution of the termination loss. The impedance of each waveguide was experimentally determined from the Smith chart to be within 10% of the 50Ω target at frequencies below 1 GHz.

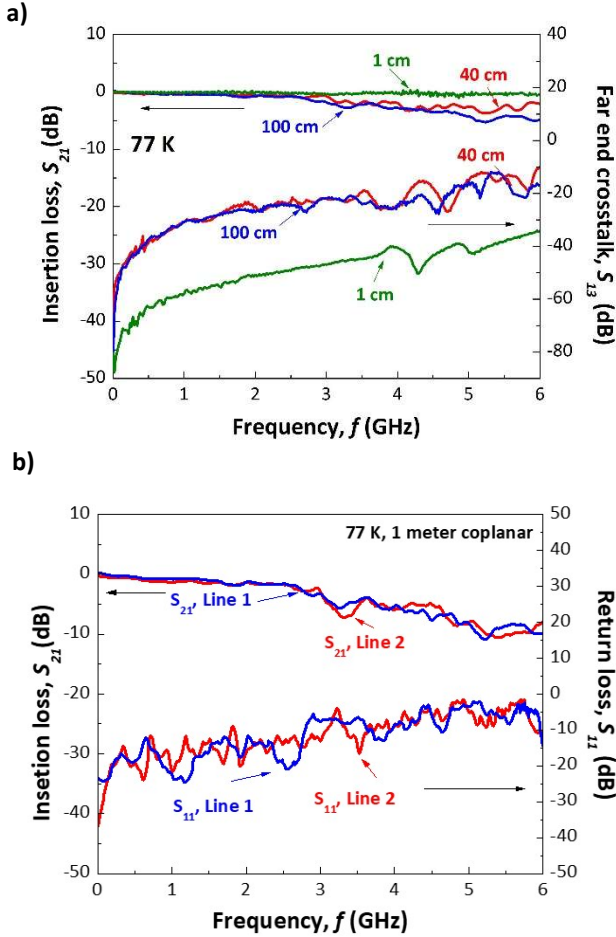


Fig. 4. a) Insertion loss and far-end cross-talk of coplanar waveguides 1, 40 and 100 cm long waveguides at 77 K. b) Insertion and return loss frequency responses of the two lines of a 1 m long coplanar waveguide.

Fig. 4b is a frequency dependence of insertion and return loss of the two lines of a 1 m long waveguide at 77 K. The S_{21} parameters of the lines are reproducible within 1 dB of each other. Out of eight 1 m long waveguides manufactured using this process, only one had a loss higher than 10 dB, which is explained by the presence of a YBCO defect in the signal line. Fig. 4b also indicates that the onset of high return loss of the waveguides and loss of impedance matching partially explains the performance degradation of the 100 cm long waveguide at frequencies higher than 3 GHz.

Fig. 5 summarizes the length dependence of the waveguide loss at 5 and 10 GHz. The solid lines are linear fits, yield loss per unit

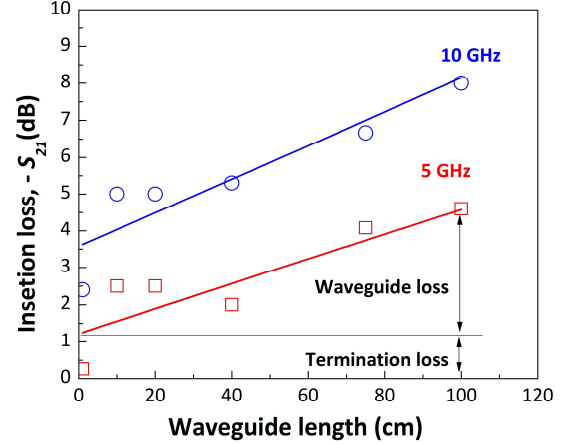


Fig. 5. Length dependences of waveguide losses at 5 and 10 GHz, 77 K. The solid lines are linear fits used to determine the signal attenuation per unit length.

length α : α (5 GHz) = 3.5 ± 0.9 dB, and α (10 GHz) = 4.4 ± 1.0 dB/m. Losses in the terminations are 1.2 and 3.5 dB at 5 and 10 GHz, correspondingly. By using the following formulas, we can estimate the contribution of the dielectric α_d :

$$\alpha_d (\text{dB/m}) \cong \frac{27.3}{\lambda_0} \sqrt{\epsilon_r} \tan(\delta) \quad (1)$$

and conduction loss α_c [10]:

$$\alpha_c (\text{dB/m}) \cong 8.68 R_s / Z_0 w \quad (2)$$

Where $\epsilon_r = 3.2$ is the dielectric constant of the Kapton support, $\tan(\delta)$ is the loss tangent of Kapton, R_s is the surface resistance of YBCO at 77 K, $w = 0.6$ mm (see also Fig. 3a) width of the signal line, and $Z_0 = 50 \Omega$ is the waveguide impedance. Using the published RF loss studies of commercial conductors [11-13], we estimate $R_s(77 \text{ K}, 5 \text{ GHz}) \approx 1 \text{ m}\Omega$ for SuperPower tape. According to Eq. 2, the predicted conduction loss $\alpha_c \approx 0.3$ dB/m is much lower than the observed values in Fig. 4a.

There is limited data on cryogenic RF losses in Kapton, and the only published study was by Harris *et al.* [14], provides $\tan(\delta) = 0.006$ at 77 K, 6 GHz. Using these values in Eq. 1, we arrive at $\alpha_d \approx 5.8$ dB/m, which is close to the experimentally observed attenuation, see Fig. 4b. The RF attenuation at 77 K in these lines is thus dominated by dielectric loss. Rujun *et al.* [15] measured quality of Kapton resonators up to 6 K and estimated that at temperatures below 4 K $\tan(\delta) < 0.001$. The projected dielectric loss contribution thus would be less than 1 dB/m at temperatures below 4 K. Other loss mechanisms, such as radiation, may dominate the waveguide attenuation at these temperatures.

Fig. 6 is a frequency response of a stand-alone 6 GHz low-pass filter, and a filter integrated with a 15 dB attenuator. The integrated filter/attenuator demonstrates a 6 ± 0.1 GHz cut-off frequency and a stop-band rejection of 30 dB. The S_{21} variations below the cut-off are explained by the lack of shielding in the coplanar geometry. A fully shielded stripline filter is expected to deliver a more consistent response.

The waveguides studied here were assembled using liquid epoxy Stycast 1266, which has a long record of excellent cryogenic performance. The flexible electronic industry is predominantly using dry-film adhesives. The dry-film adhesives

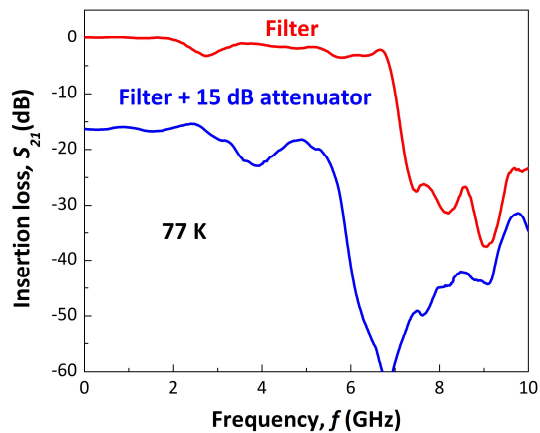


Fig. 6. Frequency response of a stand-alone low-pass 6 GHz filter and a 6GHz filter coupled with 15 dB surface-mounted attenuator.

are compatible with rapid through-put industrial lamination. In this study, we explored the possibility of using the popular b-staged adhesives offered by DuPont: acrylic-based Puralux LF and epoxy-based Puralux HP products. The adhesives are

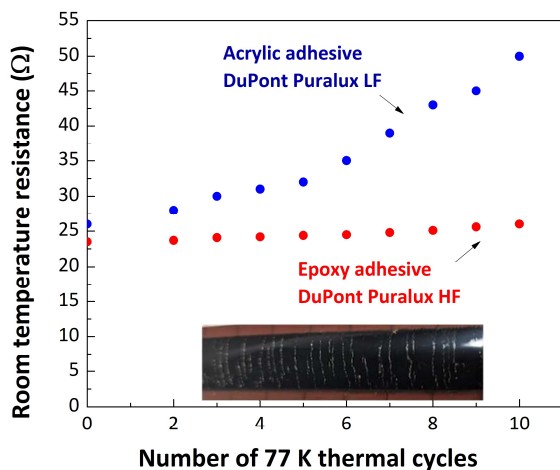


Fig. 7. Thermal cycling of laminates manufactured using b-staged acrylic adhesive DuPont Puralux LF and epoxy adhesive Puralux HF.

delivered as 25 – 50 μm thick sheets. The manufacturer recommends curing at a temperature range of 180°C – 200°C under pressure over 1 MPa. The YBCO is found to react with the adhesive at temperatures exceeding 180°C with a loss of superconductivity. The curing temperature was therefore reduced to 170°C, which did not compromise the bond strength. After the bonding and removal of metallization, the YBCO film appears intact. However, after the repeated cycling of the laminates between 77 K and room temperature, the acrylic adhesive fails, as evidenced by the increase of the normal-state resistivity, Fig. 7. Visual inspection reveals multiple cross-wise cracks, see inset in Fig. 7. At the same time, epoxy adhesive supported the YBCO film without cracking.

The problem with the dry-film adhesives is that they have a lower elastic modulus than 1266 epoxy, thus sometimes being unable to sustain the built-in stress of YBCO film after the

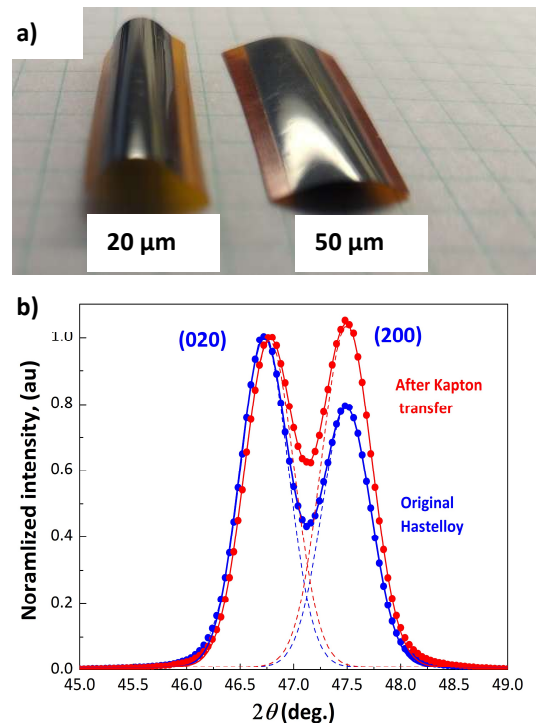


Fig. 8. a) Curling of the Kapton support by the compressive strain of YBCO film. b) In-plane X-ray diffraction of YBCO film before and after transfer to Kapton. The spectrum shows a partial de-twinning process.

metallization is etched away. After the metallization removal, the YBCO film, initially supported by a copper layer with an elastic modulus of 120 GPa, is supported by the Kapton-adhesive laminate with an elastic modulus of less than 2 GPa. The strain release is evident by the extreme curling of the laminate after the copper layer removal; see Fig. 8a.

In-plane X-ray diffraction of the YBCO film before and after transfer to Kapton confirms the significant strain release, Fig. 8b. The detail of (200) – (020) peaks shows the normal twinning pattern. After transfer to Kapton, (200) twinning orientation becomes dominant, indicating a de-twinning process, where the twin boundary motion partially releases strain. Based on these data, we estimate the built-in compressive stress on the order of ≈ 500 MPa. An adhesive that combines high elastic modulus and high adhesion strength would support such a strained film. Unfortunately, popular acrylic adhesives are not suitable for this purpose, most likely due to the low elastic modulus. High-performance dry epoxies appear to be more promising.

Alternatively, the compressive strain can be reduced by growing YBCO at a lower deposition rate than is currently employed by the 2G conductor manufacturers. A larger-grain YBCO film is expected to have a lower level of grain boundary compression and, consequently, lower internal strain.

CONCLUSION

In conclusion, we demonstrated up to 1-meter-long YBCO-Kapton waveguides. The waveguide RF attenuation is dominated by dielectric loss in the Kapton support. Future work will focus on refining the dry adhesive lamination methods that enable structurally sound scalable multi-layer YBCO architectures.

REFERENCES

- [1] M. Kjaergaard, M. E. Schwartz, J. Braumüller, P. Krantz, J. I. J. Wang, S. Gustavsson, and W. D. Oliver, "Superconducting Qubits: Current State of Play," in *Annual Review of Condensed Matter Physics, Vol 11, 2020*, vol. 11, M. C. Marchetti and A. P. Mackenzie Eds., (Annual Review of Condensed Matter Physics, 2020), pp. 369-395.
- [2] J. C. Bardin, D. H. Slichter, and D. J. Reilly, "Microwaves in Quantum Computing," *IEEE Journal of Microwaves*, vol. 1, no. 1, pp. 403-427, 2021, doi: 10.1109/JMW.2020.3034071.
- [3] V. Solovyov, H. Kim, and P. Farrell, "Multi-Line Superconducting Waveguides Based on YBCO-on-Kapton Technology," *IEEE Trans. Appl. Supercond.*, vol. 34, no. 3, pp. 1-5, 2024, doi: 10.1109/TASC.2023.3347187.
- [4] V. Solovyov, H. Kim, and P. Farrell, "High-Temperature Superconducting Interconnects for Ultra-Low Temperature, High-Field Environments," *IEEE Trans. Appl. Supercond.*, vol. 33, no. 5, pp. 1-5, 2023, doi: 10.1109/TASC.2023.3241264.
- [5] J. W. Ekin, T. M. Larson, N. F. Bergren, A. J. Nelson, A. B. Swartzlander, L. L. Kazmerski, A. J. Panson, and B. A. Blankenship, "High T_c superconductor/noble-metal contacts with surface resistivities in the $10^{-10} \Omega\text{cm}^2$ range," *Appl. Phys. Lett.*, vol. 52, no. 21, pp. 1819-1821, 1988. [Online]. Available: <http://link.aip.org/link/?APL/52/1819/1>.
- [6] V. Selvamanickam, Y. Chen, I. Kesgin, A. Guevara, T. Shi, Y. Yao, Y. Qiao, Y. Zhang, Y. Zhang, G. Majkic, G. Carota, A. Rar, Y. Xie, J. Dackow, B. Maiorov, L. Civalé, V. Braccini, J. Jaroszynski, A. Xu, D. Larbalestier, and R. Bhattacharya, "Progress in Performance Improvement and New Research Areas for Cost Reduction of 2G HTS Wires," *IEEE Trans. Appl. Supercond.*, vol. 21, no. 3, pp. 3049-3054, Jun 2011, doi: 10.1109/tasc.2011.2107310.
- [7] J. Bang, G. Bradford, K. Kim, J. Lee, A. Polyanskii, and D. Larbalestier, "Elastic-plastic conductor damage evaluation at over 0.4% strain using a high-stress REBCO coil," *Supercond. Sci. Technol.*, vol. 37, no. 9, p. 095011, 2024/08/12 2024, doi: 10.1088/1361-6668/ad6a9d.
- [8] S. Furtner, R. Nemetschek, R. Semerad, G. Sigl, and W. Prusseit, "Reel-to-reel critical current measurement of coated conductors," *Supercond. Sci. Technol.*, vol. 17, no. 5, p. S281, 2004/03/30 2004, doi: 10.1088/0953-2048/17/5/037.
- [9] V. Solovyov and P. Farrell, "Exfoliated YBCO filaments for second-generation superconducting cable," *Supercond. Sci. Technol.*, vol. 30, no. 1, p. 014006, 2017. [Online]. Available: <http://stacks.iop.org/0953-2048/30/i=1/a=014006>.
- [10] R. A. Pucel, D. J. Masse, and C. P. Hartwig, "LOSSES IN MICROSTRIP," *Ieee Transactions on Microwave Theory and Techniques*, vol. MT16, no. 6, pp. 342-&, 1968, doi: 10.1109/tmmt.1968.1126691.
- [11] P. Krkotić, A. Romanov, N. Tagdulang, G. Telles, T. Puig, J. Gutierrez, X. Granados, S. Calatroni, F. Perez, M. Pont, and J. M. O'Callaghan, "Evaluation of the nonlinear surface resistance of REBCO coated conductors for their use in the FCC-hh beam screen," *Supercond. Sci. Technol.*, vol. 35, no. 2, p. 025015, 2022/01/07 2022, doi: 10.1088/1361-6668/ac4465.
- [12] A. Romanov, P. Krkotić, G. Telles, J. O'Callaghan, M. Pont, F. Perez, X. Granados, S. Calatroni, T. Puig, and J. Gutierrez, "High frequency response of thick REBCO coated conductors in the framework of the FCC study," *Scientific Reports*, vol. 10, no. 1, p. 12325, 2020/07/23 2020, doi: 10.1038/s41598-020-69004-z.
- [13] J. Wosik, J. Krupka, K. Qin, D. Ketharnath, E. Galstyan, and V. Selvamanickam, "Microwave characterization of normal and superconducting states of MOCVD made YBCO tapes," *Supercond. Sci. Technol.*, vol. 30, no. 3, p. 035009, 2017/01/25 2017, doi: 10.1088/1361-6668/aa52a4.
- [14] A. I. Harris, M. Sieth, J. M. Lau, S. E. Church, L. A. Samoska, and K. Cleary, "Note: Cryogenic microstripline-on-Kapton microwave interconnects," *Rev. Sci. Instrum.*, vol. 83, no. 8, 2012, doi: 10.1063/1.4737185.
- [15] B. Rujun, G. A. Hernandez, C. Yang, J. A. Sellers, C. D. Ellis, D. B. Tuckerman, and M. C. Hamilton, "Cryogenic microwave characterization of Kapton polyimide using superconducting resonators," in *2016 IEEE MTT-S International Microwave Symposium (IMS), 22-27 May 2016 2016*, pp. 1-4, doi: 10.1109/MWSYM.2016.7539977. [Online]. Available: https://ieeexplore.ieee.org/stampPDF/getPDF.jsp?tp=&ar_number=7539977&ref=